International Journal of Clinical Oncology and Cancer Research
2020; 5(3): 56-64
http://www.sciencepublishinggroup.com/j/ijcocr
doi: 10.11648/j.ijcocr.20200503.12
ISSN: 2578-9503 (Print); ISSN: 2578-9511 (Online)

Novel Targets of Protoporphyrin-IX Determined By Gene Expression Analysis

Yiyang Dai[1], Wolfgang Kemmner[2, *]

[1]Department of Gastroenterology, The Fourth Affiliated Hospital of Zhejiang University School of Medicine, Yi Wu, China

[2]Research Group Translational Oncology, Experimental Clinical Research Center at the Max-Delbrueck-Center for Molecular Medicine, Charitè Campus Buch, Berlin, Germany

Email address:
wkemmner@mdc-berlin.de (W. Kemmner)

[*]Corresponding author

To cite this article:
Yiyang Dai, Wolfgang Kemmner. Novel Targets of Protoporphyrin-IX Determined By Gene Expression Analysis. *International Journal of Clinical Oncology and Cancer Research*. Vol. 5, No. 3, 2020, pp. 56-64. doi: 10.11648/j.ijcocr.20200503.12

Received: July 8, 2020; **Accepted**: July 27, 2020; **Published**: August 18, 2020

Abstract: Treatment with 5-Aminolevulinic acid-mediated photodynamic therapy is a promising therapeutic option for various carcinomas. An appropriate photosensitizer for photodynamic therapy is protoporphyrin-IX (PpIX), a light sensitive metabolite of heme synthesis. Incorporation of iron into PpIX leading to heme is carried out by Ferrochelatase (FECH). Earlier, we described a significant down regulation of FECH mRNA-expression and enzyme activity in carcinoma cells leading to an endogenous accumulation of PpIX. How PpIX affects the cell metabolism has not been examined so far. Thus, we tried to identify novel targets of PpIX with regard to cell proliferation, apoptosis and invasion. Endogenous generation of PpIX was induced by silencing of FECH in breast carcinoma MDA-MB-231 cells using a specific siRNA. Successful silencing of FECH was confirmed by RT-PCR and induction of PpIX was assessed by flow cytometry for each experiment. Subsequently, gene expression was determined using Affymetrix GeneChip® Human Gene 1.0 ST. Validation of microarray data was achieved by quantitative RT-PCR. Expression of one of the newly discovered target genes, BAMBI, was assessed by immunohistochemistry. In addition, the effect of silencing of FECH was examined by functional studies of cell apoptosis, invasion and wound healing. According to the gene expression analysis, an enhancement of PpIX suppressed Hedgehog as well as TGF-beta signaling. Expression of HHIP, a negative regulator of the hedgehog pathway, was found to be strongly increased after silencing of FECH. With regard to TGF-beta signaling, expression of the signaling inhibitor SMAD7 was strongly upregulated while the positive mediators SMAD2 and SMAD4 were less expressed after silencing FECH. Similarly, apoptosis of tumor cells was promoted, probably due to an increased expression of the pro-apoptotic gene APAF1 and a reduced expression of anti-apoptotic protein API5. Moreover, a significantly reduced invasion capability after treatment of cells with FECH siRNA was found. Here, we report that an accumulation of PpIX due to silencing of FECH affects various pathways and promotes apoptosis of tumor cells in different ways. Thus, silencing of FECH might have a tumor-suppressive effect. The search for substances which block FECH activity in a direct way therefore might be of high relevance for future cancer therapy approaches.

Keywords: Photodynamic Therapy, Protoporphyrin-IX, Ferrochelatase, Silencing RNA, Microarray, Gene Expression, Apoptosis, Invasion

1. Introduction

Photodynamic therapy (PDT) is a promising approach for improved cancer treatment. PDT treatment has important advantages, because it is noninvasive with short treatment times, has a high repeatability without side effects, and shows little or no scar after healing. An appropriate photosensitizer for PDT is protoporphyrin IX (PpIX), a light sensitive metabolite of heme synthesis (1). Generation of PpIX depends on a sufficient intracellular delivery of the precursor substance aminolevulinic acid (ALA). Ferrochelatase FECH (EC 4.99.1.1) is responsible for the last step of heme-synthesis, incorporation of iron into PpIX

leading to heme. After activation by light, PpIX induces the generation of reactive oxygen species responsible for cellular oxidation and subsequent tumor cell death. In previous studies, we found a significant down regulation of FECH mRNA-expression and enzyme activity in gastrointestinal carcinomas leading to an endogenous accumulation of PpIX within the tumor cells (2, 3). Through inhibition of FECH mRNA expression using a specific siRNA-based probe we were able to amplify the specific endogenous fluorescence emission of PpIX within cancerous tissue. Successful induction of PpIX by silencing FECH was demonstrated e.g. by flow cytometry (4).

PpIX is also an activator of p53 and TAp73α tumor suppressors (5, 6). According to the results of Zawacka-Pankau J et al. direct binding of PpIX to N-terminal regions of p53 and p73 can release these tumor suppressors from e.g. inhibition by MDM2. Reactivation of tumor suppressors might promote a massive cancer cell death after photodynamic treatment. Moreover, PpIX has been described to target tumor suppressors directly (7). Recently, Lee JM et al. have discovered that PpIX treatment is able to increase miR-199a-5p levels leading to the inhibition of various EMT-targets (8).

The aim of this paper was to identify novel targets of PpIX. Here, we present the first comprehensive gene expression study of the effects of an intracellular accumulation of PpIX in cancer cells. To this end, endogenous generation of PpIX was induced by treating breast carcinoma MDA-MB-231 cells with a specific FECH siRNA. Silencing of FECH was demonstrated by RT-PCR and successful induction of PpIX was assessed by flow cytometry for each experiment as described in (4). Subsequently, a microarray study of the gene expression was performed using Affymetrix GeneChip® Human Gene 1.0 ST. Validation of microarray data was achieved by quantitative RT-PCR of six genes. Expression of one of the newly discovered target genes, BAMBI, was assessed by immunohistochemistry. In addition, the effect of silencing of FECH was examined by functional studies of cell apoptosis, invasion and wound healing. The results show that an accumulation of PpIX due to silencing of FECH affects various pathways and promotes apoptosis of tumor cells in different ways. Moreover, we found a significantly reduced invasion capability after treatment of cells with FECH siRNA. In summary, intracellular accumulation of PpIX seems to have a tumor-suppressive effect.

2. Methods

2.1. Study Design and Gene Expression Analysis

Breast cancer cells MDA-MB-231 were divided into four treatment groups. For promoting the activity of heme metabolism, aminolevulinic acid (5-ALA) was added to all experimental groups except group D, which was a no treatment group. For silencing of FECH a specific siRNA described earlier was used (3). For comparison a control siRNA, Allstar siRNA, was applied. In each case, silencing of FECH was checked by RT-PCR and successful induction of PpIX was assessed by flow cytometry (see below). Gene expression was studied using Affymetrix GeneChip® Human Gene 1.0 ST.

Experimental details: Group A) are cells treated with 15 nM FECH siRNA + 0.1 mM 5-ALA; B) is a control group of cells which was treated with 15 nM Allstar siRNA + 0.1 mM 5-ALA; C) Cells were treated only with 0.1 mM 5-ALA but no siRNA; D) is an additional no treatment group. After treatment RNA was extracted as described below. The four treatment groups were analyzed three times in an independent fashion. Thus, twelve microarrays were examined. Preparation of labelled cRNA and hybridization was done according to the manufacturer's instructions using the Gene Chip Hybridization, Wash and Stain Kit (Affymetrix, Santa Clara, CA). Except the common quality control provided by gene chip operating software, a scientific workflow for chip quality control was set up in our lab including pseudo image plots, scatter MA plot and relative log expression plot. The resulting microarray data were preprocessed using the robust multichip average (RMA) algorithm via the BioConductor oligo package (9). Gene expression of FECH siRNA-treated cells was compared with that of the cells transfected with control siRNA by calculating the ratio of the signal intensity of FECH siRNA-transfected cells vs. the signal intensity of the control-transfected cells. A list of all the genes included in these microarrays and the normalized data have been deposited in the Gene Expression Omnibus database (http://www.ncbi.nlm.nih.gov/geo/info/linking.html) under GEO accession number GSE135845.

2.2. Cell Culture

The human breast carcinoma cell line MDA-MB-231 (HTB 26; American Type Culture Collection) was grown in monolayer cultures in RPMI medium supplemented with 10% fetal calf serum (FCS), 2 mM glutamine. MDA-MB-231 breast cancer cells harbor mutant p53 (10). Gastric carcinoma cells MKN28 (ATCC) were kept in DMEM low Glucose (Invitrogen, Karlsruhe Germany), 10% FCS, 2mM Glutamine. MKN28 contain point mutations of the p53 gene (11). Human fibrosarcoma cells HT-1080 (ATCC) were grown in in DMEM (Invitrogen, Karlsruhe Germany), 10% FCS, 1% NEAS and 1% Na-pyruvate. HT-1080 fibrosarcoma cells are a classic ferroptosis model that express wild-type p53 (12). All cell lines were cultured in a humidified atmosphere containing 5% CO_2, 37°C.

2.3. Transient siRNA Transfection

All siRNA-molecules were designed according to standard procedures and obtained from Qiagen (Hilden, Germany). For silencing FECH the following sequence was used: siRNA FECH, 5'- gaauauccucuugguuccg -3', covering the FECH mRNA, transcript variant 1, with accession

NM_001012515.1. The efficiency of this sequence has been confirmed earlier (3). As negative control Allstars siRNA was used. AllStars Negative Control siRNA has been validated using Affymetrix GeneChip arrays and a variety of cell-based assays and was shown to ensure minimal nonspecific effects on gene expression and phenotype. Cloning experiments confirmed that AllStars Negative Control siRNA enters RISC (see Qiagen, Hilden, Germany). For transfection, cells were seeded at a cell density of $1x10^5$ cells/well in a 6-well plate and cultivated for 24 hours in DMEM medium with FCS. Then, 198 µl DMEM cell culture medium was added to 2 µl FECH siRNA or control siRNA. Another 196 µl DMEM cell culture medium was added to 4 µl Dharmafect, incubated for 5 min at RT, mixed carefully with the siRNA solution and kept for another 20 min at RT. These 400 µl of the siRNA-containing solution were added to 1600 µl medium, resulting in a siRNA concentration of 15 nM. Cells were incubated for 72 hours in the siRNA transfection solution. After washing, cells were incubated for another 24 hours in DMEM medium without FCS. Generation of PpIX was promoted by subsequently incubation of the cells with 0.1 mM 5-ALA for 3 h at 37°C. In each case, silencing of FECH was checked by RT-PCR and successful induction of PpIX was assessed by flow cytometry. PpIX-fluorescence was detected with a BD Fortressa flow cytometer at an excitation of 405 nm and an emission of 635 nm as described (4).

2.4. RNA Extraction and RT-PCR

RNA extractions were carried out using RNeasy Mini Kit (Qiagen, Valencia, CA) following the manufacturer's instructions. Total RNA quality and yield were assessed using a bioanalyzer system (Agilent 2100 Bioanalyzer; Agilent Technologies, Palo Alto, CA) and a spectrophotometer (NanoDrop ND-1000; NanoDrop Technologies, Wilmington, DE). Only RNA with an RNA Integrity Number (RIN) above 9.0 was used for further analysis. For quantification of the expression levels of various genes as found by microarray, RT-PCR was performed using pre-designed gene-specific TaqMan® probes and primer sets purchased from Applied Biosystems (Table 1). RT-PCR amplification was carried out using RNA UltraSense One-Step Quantitative RT-PCR System (Invitrogen) on an ABI PRISM 7900HT Sequence Detection System with fluorescence detection (Applied Biosystems), according to the manufacturer's instructions. Quantitative RT-PCR was run under the following conditions: 50°C for 15 minutes, 95°C for 2 minutes, followed by 40 cycles of 95°C for 15 seconds, and 60°C for 1 minute. All samples were amplified in triplicate reactions. Gene expression was quantified relative to the expression of internal control ß-Actin using Sequence Detector Software (SDS 2.2, Applied Biosystems) and the relative quantification method for quantitative RT-PCR. In addition, ß-Actin levels were used to determine whether a given sample contained sufficient mRNA to be included in the study. Samples for which the Ct value for ß-Actin was above 22 were excluded from the analysis. The relative expression of each individual gene was calculated based on the determined Δ^{CT} values. The Δ^{CT} value is the difference between the Ct value for an individual gene and the internal reference control gene (13). Δ^{CT} values correspond to a log (-2) scale. The result of quantitative gene expression was calculated as a $2^{-}\Delta^{CT}$ relative to ß-Actin expression in the corresponding samples (14). Gene expression of FECH siRNA-treated cells was compared with that of the cells transfected with control siRNA by calculating the ratio of the relative amount of FECH siRNA-transfected cells vs. the relative amount of the control-transfected cells.

Table 1. *Assays-on-Demand for RT-PCR.*

Assay-on-Demand	Gene	Description
Hs03023880_g1	ACTB	ß-Actin
Hs00610320_m1	TGFBR1	Transforming growth factor, beta receptor I
Hs00183425_m1	SMAD2	SMAD family member 2
Hs00998193_m1	SMAD7	SMAD family member 7
Hs00172878_m1	HES1	Hairy and enhancer of split 1
Hs01011015_m1	HHIP	Hedgehog interacting protein
Hs01119974_m1	GLI3	GLI family zinc finger 2
Hs00164616_m1	FECH	Ferrochelatase

Table 1 For quantification of mRNA-expression, specific Assays-on-Demand, designed and produced by Applied Biosystems (Weiterstadt, Germany) were used.

2.5. Determination of Apoptosis of Breast Carcinoma Cells by Flow Cytometry

Apoptosis was determined using an Annexin V-FITC detection kit (BD Biosciences, CA) according to the manufacturer's instructions. For flow cytometric analysis, at least 10,000 MDA-MB-231 breast cancer cells were evaluated using a FACSCalibur (BD Biosciences, CA). Cell cycle distribution and pre-G1 fraction were determined in a quantitative way using the CellQUEST™ program. Annexin V positive-propidium iodide (PI) negative cells were counted as early apoptotic cells. All experiments were done at least in triplicates.

2.6. Detection of BAMBI Expression of Gastric Cancer Cells by Flow Cytometry

Harvest, wash the cells and adjust cell suspension to a concentration of $2.5x10^5$ cells/ml in ice cold PBS, 10% FCS, 1% sodium azide. Add 2.5 µg/ml of primary antibody or isotype control antibody. Primary antibody for BAMBI detection was a mouse monoclonal (ab57043 from Abcam, Berlin, Germany). Isotype control was a monoclonal Mouse IgG1 (ab170190, Abcam). Cells were incubated overnight in the dark at 4°C. Cells were washed by centrifugation at 400 g for 7 min and resuspended in 100 µl ice cold PBS, 10% FCS, 1% sodium azide. Addition of secondary antibody (10 µg/ml) was followed by incubation 60 min at room temperature. Secondary antibody was a Goat Anti-Mouse IgG H&L-Alexa Fluor® 488 preadsorbed (ab150117, Abcam). Cells were washed by centrifugation at 400 g for 7 min and resuspended in 300 µl Stain-buffer (BD Biosciences, CA). For flow cytometric analysis, at least 10,000 cells were evaluated using a FACSCalibur ™ (BD Biosciences, CA).

2.7. Invasion Assay

Fibrosarcoma cells HT 1080 were treated with FECH siRNA as described above. Bio Coat Matrigel Invasion Chambers (Corning, USA) were used according to the instructions of the manufacturer. Briefly, $1x10^5$ pretreated cells were seeded into the insert chambers, and the cells there were kept in DMEM medium without FKS. The wells around the chamber contained DMEM medium with 20% FKS. After an incubation period of 24 h at 37°C within in the CO_2-incubator, non-invasive cells remaining within the chamber insert or invasive cells sitting at the bottom of the well were dissolved by careful treatment with the enzyme Accutase (Sigma-Aldrich, USA). Cells from each fraction were collected separately and cell number and viability were counted using a Cellometer Vision device and manually. As the last step, RNA was isolated and successful transfection with FECH siRNA was determined by quantitative PCR (see above).

2.8. Wound-Healing Assay

For wound healing assays, MDA-MB-231 cells treated with siFECH (see above) were used. Experiments were performed in triplicates using ibidi Culture–Inserts (ibidi, Munich, Germany). The inserts create a wound field with a defined gap of 9 mm x 9 mm for measuring the migratory and proliferation rates of cells. Migratory cells are able to extend protrusions and ultimately invade and close the wound field. Cells were seeded at a cell density of $5x10^5$ cells/well in a 6-well plate and cultivated for 24 hours at 37°C and 5% CO_2. One insert per well was transferred with sterile tweezers into a 24 well plate. The original cell solution was diluted to $1x10^6$ cells per ml and 70 µl of the solution was added into each chamber of the insert. Wells were filled up with 1ml cell culture medium and plates were incubated overnight at 37°C and 5% CO_2. Then the inserts were removed from the wells. Cell proliferation and migration after various incubation times was checked by microscopy.

2.9. Immunohistochemical Detection of BAMBI Expression

Immunohistochemistry was performed on 10 µm thin cryosections mounted on SuperFrost®Plus microscope slides (Menzel GmbH & Co KG, Braunschweig, Germany). MDA-MB-231 cells were treated as described above. Successful transfection with FECH siRNA was determined by quantitative PCR. Cells were fixed with 4% paraformaldehyde for 10 min and then permeabilized with 0.1% PBS-Tween for 20 min. Cells were then incubated in 10% normal goat serum / 0.3M glycine in PBS to block non-specific protein-protein interactions. Primary antibody for BAMBI detection was a mouse monoclonal (ab57043, Abcam) ($1µg/1x10^5$ cells). Incubation was for 30 min at RT. Following washes in PBS, sections were incubated with secondary antibody Goat Anti-Mouse IgG H&L, Alexa Fluor® 488 preadsorbed (ab150117, Abcam) at 1/500 dilution for 30 min at RT. Microscopic pictures were taken using an inverted confocal laser scanning microscope Zeiss LSM710.

2.10. Statistical Analysis

Statistical calculation was done using GraphPad Prism version 5 for Windows (GraphPad Software).

3. Results & Discussion

3.1. Gene Expression of Heme Metabolism Enzymes After ALA-addition or Silencing of FECH

In a first approach the effects of silencing Ferrochelatase FECH (EC 4.99.1.1) on expression of the enzymes of heme biosynthesis was examined. FECH is responsible for the last step of heme-synthesis, incorporation of iron into PpIX. FECH down regulation and loss of enzymatic activity corresponds clearly with enhanced PpIX-dependent fluorescence (4). In addition, enhanced production of PpIX depends on a sufficient intracellular delivery of the precursor substance 5'-aminolevulinic acid (5-ALA). Heme biosynthesis is controlled by the rate of the initial enzyme, mitochondrial 5'-aminolevulinate Synthase 1 (ALAS1), which is under negative-feedback regulation by heme itself. Heme blocks transcription of the ALAS1 gene and stimulates the rate of degradation of the specific mRNA (15). Another essential enzyme in heme catabolism is heme oxygenase (HMOX). This enzyme cleaves heme to form biliverdin, carbon monoxide, and ferrous iron. Two forms have been described, an inducible heme oxygenase-1 HMOX1 and a constitutive heme oxygenase-2 HMOX2 (16). HMOX1 activity is induced by the substrate heme but also by various nonheme substances.

Effects of silencing FECH on gene expression in MDA-MB-231 cells were studied by microarray analysis. In order to promote PpIX generation, 5-ALA was added in all treatment groups except group D (no treatment group). The results of the microarray study showed that addition of 5-ALA vs. no treatment leads to a 4-fold increase in HMOX1 and a strong decrease of ALAS1 (Table 2, first column). The increased expression of HMOX1 and the decreased expression of ALAS1 is what one expects due to the increased synthesis of heme after addition of 5-ALA. Treatment of cells with FECH siRNA vs control siRNA decreased FECH expression strongly as determined by gene expression analysis (Table 2, second column). Interestingly, also HMOX1 expression was reduced, probably due to the decrease in heme synthesis after silencing FECH. Thus, the results of the microarray analysis agree with the literature, confirming the quality of the microarray data.

Table 2. *Expression of enzymes of the heme metabolism.*

Heme-Synthesis	ALA vs. NTC	FECH vs. Control siRNA
ALAS1	0.59	2.18
FECH	1.01	0.25
HMOX1	4.06	0.31

Table 2 Differential expression of ALAS1, HMOX1 and FECH after addition of ALA in comparison to no treatment control (left side) or after silencing of FECH in comparison to Allstar control siRNA treatment (right side). Depicted are

the ratios of the signal intensity as found in the microarray studies (see Material& Methods section).

3.2. Effects of Enhanced PpIX on the Expression of Genes Related to Apoptosis

Silencing of FECH led to an increased expression of the pro-apoptotic genes APAF1 and BAK1 in comparison with a treatment by control siRNA (Table 3). APAF1 encodes a cytoplasmic protein that initiates apoptosis (17). BAK1 facilitates the opening of the mitochondrial voltage-dependent anion channel promoting a loss in membrane potential and the release of cytochrome c. BAK1 is also a target of p53 (18). In contrast, expression of anti-apoptotic proteins was reduced. API5 is an apoptosis inhibitory protein. API5 overexpression promotes tumor progression and suppresses apoptosis (19). In agreement, expression of the pro-apoptotic gene CASP6 was decreased. These data suggest that enhanced PpIX due to silencing FECH promotes apoptosis in several ways.

Table 3. *Differential expression of genes associated with apoptosis after silencing of FECH.*

FECH vs. Control siRNA	Gene	Description	Functional aspects
2.14	JUN	jun oncogene	JUN overexpression induced cell death and growth inhibition
1.70	APAF1	apoptotic peptidase activating factor 1	Upon binding cytochrome c this protein forms an oligomeric apoptosome
1.23	BAK1	BCL2 Antagonist/Killer 1	Pro-apoptotic regulator
0.52	API5	apoptosis inhibitor 5	Critical determinant of dE2F1-induced apoptosis in vivo and in vitro
0.49	CASP6	caspase 6, apoptosis-related cysteine peptidase	Downstream enzyme in the caspase activation cascade

Table 3 FECH vs Control siRNA: ratio of the signal intensity after silencing FECH in comparison to Allstar control siRNA treatment (see Material& Methods section).

3.3. TGF-beta Pathway Blocked by Increased PpIX Due to Silencing of FECH

According to the literature, TGF-beta is thought to be a tumor suppressor (20). TGF-beta signaling prevents growth by inducing cell cycle arrest and apoptosis through repression of cyclin dependent kinases and mitogenic c-MYC in normal epithelia and in early tumorigenic cells. However, in late stage tumorigenic cells TGF-beta stimulates cancer progression and metastasis e.g. by activation of epithelial-to-mesenchymal transition (EMT) (21). According to the microarray data, enhanced PpIX due to silencing FECH blocks TGF-beta signaling (Table 4). On the one hand, the inhibitory mediator SMAD7 was strongly upregulated. On the other hand, positive mediators SMAD2 and SMAD4 were less expressed. Upregulation of SMAD7 expression and reduced expression of TGFBR1 was confirmed by RT-PCR (Table 6). SMAD proteins are intracellular mediators of TGF-beta superfamily. SMAD7 inhibits TGF-beta signaling. Similarly, a reduced expression of CRIM1 was detected. CRIM1 promotes tumor development and progression through its potential role in EMT (22). Moreover, an enhanced expression of BAMBI (BMP and activin membrane-bound inhibitor homolog) was found by gene expression. Bambi overexpression was confirmed on the protein level by immunohistochemistry for breast carcinoma cells MDA-MB-231 and by flow cytometry for gastric carcinoma cells MKN28 (Figures 1 and 2). Recently, BAMBI overexpression was found to inhibit growth and metastasis of gastric cancer cells (23). Thus, our data suggest that PpIX reduces TGF-beta signaling and tumor cell growth.

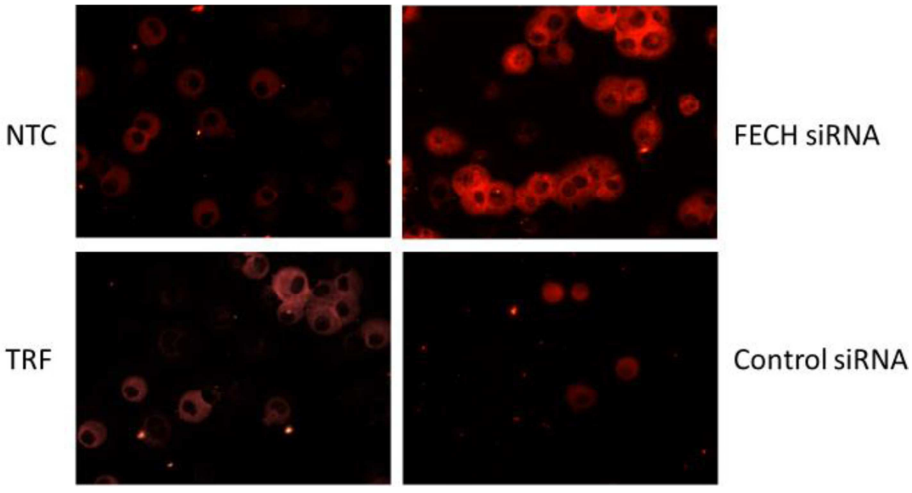

Figure 1. *Enhanced staining of BAMBI on MDA-MB-231 breast cancer cells treated with FECH siRNA.*

Abbreviations: NTC, no treatment group; TRF, Transfection reagent only; Control, treated with Allstar siRNA; FECH, treated with FECH siRNA. Briefly, immunohistochemistry was performed on 10 µm thin cryosections. MDA-MB-231 cells treated as above were fixed with 4% paraformaldehyde. For further details, please see the Materials& Methods section.

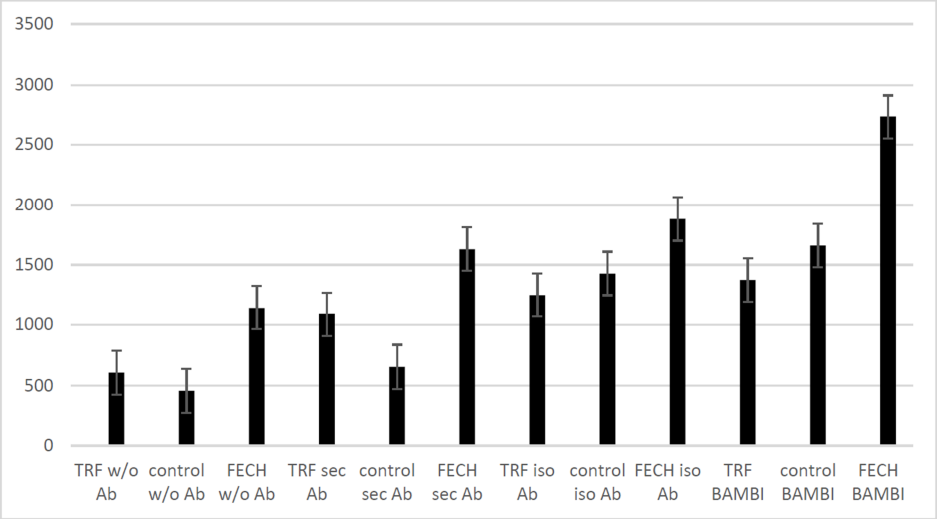

Figure 2. *Enhanced staining of BAMBI on MKN28 gastric cancer cells treated with FECH siRNA.*

FACS staining showed that BAMBI is highly expressed on MKN-28 cells treated with FECH siRNA. Abbreviations: TRF w/o Ab, transfection reagent, no antibody; control w/o Ab, control siRNA, no antibody; FECH w/o Ab, FECH siRNA, no antibody. TRF sec Ab, transfection reagent, secondary antibody; control sec Ab, control siRNA, secondary antibody; FECH sec Ab, FECH siRNA, secondary antibody. TRF iso Ab, transfection reagent, isotype antibody; control iso Ab, control siRNA, isotype antibody; FECH iso Ab, FECH siRNA, isotype antibody. TRF BAMBI, transfection reagent, BAMBI antibody; control BAMBI, control siRNA, BAMBI antibody; FECH BAMBI, FECH siRNA, BAMBI antibody.

Table 4. *Differential expression of genes associated with the TGF-beta pathway after silencing of FECH.*

FECH vs. Control siRNA	Gene	Description	Functional aspects
2.70s	SMAD7	SMAD family member 7	Inhibits TGF-beta signaling by associating with their receptors thus preventing SMAD2 access
1.41	TGIF2	TGFB-induced factor homeobox 2	Represses transcription interacting with TGF-beta activated SMAD proteins
0,10	SMAD4	SMAD family member 4	Component of the heterotrimeric SMAD2/ SMAD3- SMAD4 complex that is required for the TGF-mediated signaling
0.49	CRIM1	Cysteine-rich motor neuron1 protein	Antagonist of bone morphogenetic proteins
0.45	TGFBR1	transforming growth factor, beta receptor I	
0.39	SMAD2	SMAD family member 2	Component of the heterotrimeric SMAD2/ SMAD3- SMAD4 complex that is required for the TGF-mediated signaling

Table 4 FECH vs Control siRNA: ratio of the signal intensity after silencing FECH in comparison to Allstar control siRNA treatment (see Material& Methods section).

3.4. Hedgehog Signaling Blocked by Increased PpIX Due to Silencing of FECH

Hedgehog (HH) signaling affects cell differentiation, cell proliferation and tissue polarity, as well as the maintenance of stem cells, tissue repair, and regeneration (24). Three ligands, Indian, Sonic, and Desert HH activate this pathway. Binding of HH ligands leads to nuclear translocation of GLI transcription factors. According to gene expression analysis, silencing of FECH promoted HHIP expression (Table 5). HHIP overexpression was confirmed PCR (Table 6). HHIP functions as a negative regulator of the hedgehog pathway. Meanwhile, it has been found that HHIP-overexpression inhibits gastric carcinoma cell proliferation, migration and invasion (25). Similarly, expression of Glioma‐associated oncogene 3 (Gli3) was found to be increased by microarray data as well as by PCR. GLi3 acts as the main repressor of the pathway in the absence of HH ligands. Thus, silencing of FECH seems to block Hedgehog signaling as well as TGF-beta signaling as shown above.

Table 5. *Differential expression of genes associated with Hedgehog signaling and regulation of cell division after silencing of FECH.*

FECH vs. Control siRNA	Gene	Description	Functional aspects
4.57	HHIP	hedgehog interacting protein	Overexpression inhibits cell proliferation, migration and invasion
3.27	HES1	hairy and enhancer of split 1	Stimulates proliferation and invasion, suppresses apoptosis
2.01	GADD45A	growth arrest and DNA-damage-inducible, alpha	Inhibits entry of cells into S phase, promotes growth arrest
1.79	GLI3	GLI family zinc finger 3	GLI3 acts as the main repressor of the hedgehog pathway

Table 5 FECH vs Control siRNA: ratio of the signal intensity after silencing FECH in comparison to Allstar control siRNA treatment (see Material& Methods section).

3.5. Other Genes of Interest

Interestingly, silencing of FECH affects also WNT signaling. Lee JM et al. found that PpIX treatment increased miR-199a-5p, leading to a decreased expression of various EMT-targets (8). This micro-RNA was found to affect multiple biological processes such as cell proliferation, apoptosis, migration and invasion (26). In addition, Kim BK et al. found that miR-199a-5p interacts with Wnt/β-catenin pathway and reduces Frizzled Class Receptor 6 (FZD6) expression (27). In agreement, we found a strong downregulation of FZD6 (ratio 0.35) after silencing of FECH. This is another hint that silencing FECH/ enhanced PpIX exerts a tumor-suppressive effect. However, also an increased expression (2.05) of Cyclin D2 (CCND2) was found. CCND2 belongs to the D-type cyclin family and participates in cell cycle progression and the induction of cancer progression (28). Thus, overexpression of CCND2 as found here might have a tumor-promoting effect.

As mentioned in the introduction, Joanna Zawacka-Pankau et al. (6) have shown that PpIX induces both p53-dependent and -independent apoptosis since PpIX is an activator of p53 and TAp73α tumor suppressors. Involved in this process is early growth response 2 (EGR2) which was identified as a direct transcriptional target of p53 family and which is able to induce the p53-dependent apoptotic pathway (29). In agreement, here we found that EGR2 is strongly enhanced after silencing of FECH (ratio 2.12) and might be activated by PpIX directly.

3.6. Functional Studies

The results of the microarray study support the notion that an enhanced amount of PpIX promotes apoptosis of cancer cells (Table 2). Accordingly, the functional studies showed an increase of early apoptosis of MDA-MB-231 breast after FECH siRNA treatment (Figure 3) in comparison to cells treated with control siRNA. According to the gene expression analysis, enhanced PpIX suppresses Hedgehog as well as TGF-beta signaling. Moreover, expression of BAMBI (BMP and activin membrane-bound inhibitor homolog) which negatively regulates TGF-beta signaling was found to be enhanced. In agreement, in functional studies of MDA-MB-231 breast cancer cells treated with FECH siRNA a reduced capacity of the cells for invasion (Figure 4) and a slightly delayed capacity for wound healing was demonstrated (Figure 5).

Table 6. *Validation of gene expression found by microarray analysis by quantitative RT-PCR.*

FECH vs. Control siRNA	Gene	Description
0.99	SMAD2	SMAD family member 2
1.70	SMAD7	SMAD family member 7
1.37	HES1	Hairy and enhancer of split 1
4.44	HHIP	Hedgehog interacting protein
1.91	GLI3	GLI family zinc finger 3
0.13	FECH	Ferrochelatase

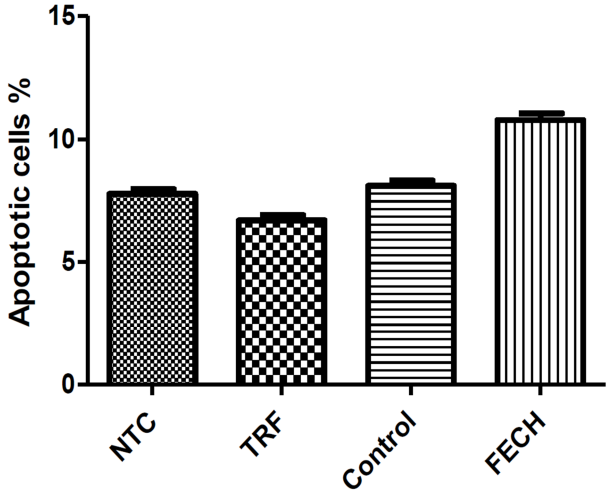

Figure 3. *FECH siRNA treatment increased apoptosis of MDA-MB-231 breast cancer cells.*

Abbreviations: NTC, no treatment group; TRF, Transfection reagent only; Control, treated with Allstar siRNA; FECH, treated with FECH siRNA (Significance $p<0.001$, t-Test of FECH vs. control siRNA). Apoptosis was determined using an Annexin V-FITC detection kit (BD Biosciences) according to the manufacturer's instructions. For flow cytometric analysis, at least 10,000 cells were evaluated using a FACSCalibur. Cell cycle distribution and pre-G1 fraction were determined in a quantitative way using the CellQUEST™ program. Annexin V positive –PI negative cells were counted as early apoptotic cells. All experiments were done in triplicates.

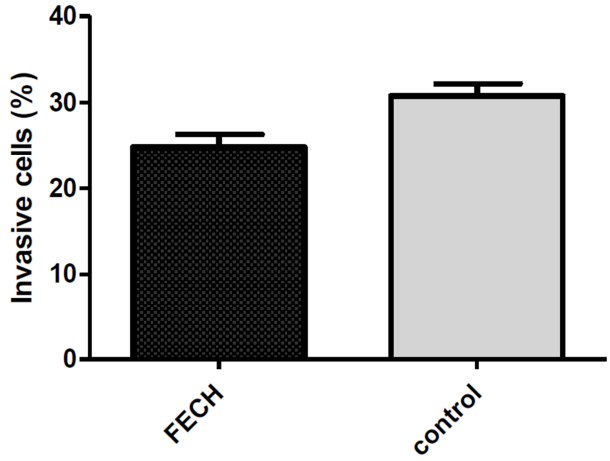

Figure 4. *Reduced invasion of cells after treatment with FECH siRNA.*

Treatment with FECH siRNA significantly ($p<0.02$) reduced the invasive capacity of cancer cells. Invasion was examined as described in Materials& Methods section. Briefly, Matrigel Invasion Chambers (Corning, USA) were used according to the instructions of the manufacturer. Briefly, $1x10^5$ cells were seeded into the insert chambers, and the cells there were kept in DMEM medium without FKS. The wells around the chamber contained DMEM medium with 20% FKS. After an incubation period of 24 h at 37°C within in the CO_2-incubator, non-invasive cells remaining within the chamber insert or invasive cells sitting at the bottom of the well were dissolved by careful treatment by enzyme treatment. Cells from each fraction were collected separately and cell number and viability. As the last step, RNA was isolated and successful transfection with FECH siRNA was determined by quantitative PCR.

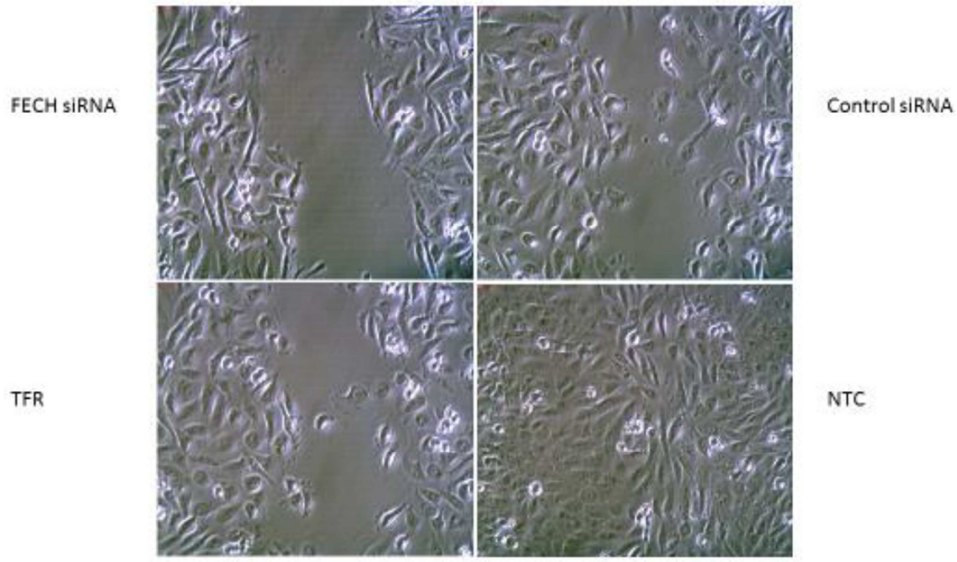

Figure 5. *Treatment with FECH siRNA delayed wound healing and reduced migration.*

Representative images were taken at 8 hours post-scratch. Wound healing assays were performed four times. Wound healing of cells treated with FECH siRNA was delayed, but significance was not reached. Wound healing was examined as described in Materials& Methods section. Abbreviations: NTC, no treatment group; TRF, Transfection reagent only; Control, treated with Allstar siRNA; FECH, treated with FECH siRNA.

Table 6 Gene expression of FECH siRNA-treated breast carcinoma cells MDA-MB-231 cells was compared with that of cells transfected with Allstar control siRNA by calculating the ratio of the relative amount of FECH siRNA-transfected cells vs. the relative amount of the control-transfected cells (Material& Methods section). FECH vs Control siRNA: Fold change of expression after silencing FECH by specific siRNA in comparison to Allstar siRNA.

4. Conclusion

The aim of this study was the generation of a database that allows the identification of genes or groups of genes, which show an altered expression after increasing PpIX intracellularly. In contrast to other investigations, PpIX was not added to the cell culture medium directly, however the concentration of endogenous PpIX was increased through silencing of FECH. This increase was confirmed for each experiment by flow cytometry of fluorescent PpIX. An enhanced expression of PpIX due to a silencing of FECH seems to affect the properties of cancer cells in several ways. Both gene expression analysis and functional assays suggest that an enhanced amount of PpIX promotes apoptosis of cancer cells. Moreover, according to the microarray results, HHIP and SMAD7 are important effector molecules for the modified functional characteristics of cells treated with FECH siRNA. Future studies will show how PpIX affects apoptosis and invasion by controlling gene expression of these mediator molecules. Another important aspect is that an enhanced amount of PpIX seems to have a tumor-protective or suppressive effect on breast cancer cells. Therefore, the search for substances that block FECH activity directly might be of considerable relevance for future cancer therapy approaches.

Authors' Contributions

YD performed the analysis, interpreted the results and wrote the manuscript. WK designed the study, provided critical analysis of the manuscript, assisted with the statistical analysis, and revised the manuscript for important intellectual content. All authors critically analyzed, read and approved the final manuscript.

Funding

Zhejiang Provincial Natural Science Foundation supported our project # LY15H030010.

Competing Interests

The authors declare that they have no competing interests.

Acknowledgements

The authors thank Mrs. Sabine Grigull and Mrs. Gudrun Koch for excellent technical assistance.

References

[1] Ishizuka M, Abe F, Sano Y, Takahashi K, Inoue K, Nakajima M, et al. Novel development of 5-aminolevurinic acid (ALA) in cancer diagnoses and therapy. Int Immunopharmacol. 2011; 11 (3): 358-65.

[2] Moesta KT, Ebert B, Handke T, Nolte D, Nowak C, Haensch WE, et al. Protoporphyrin IX occurs naturally in colorectal cancers and their metastases. Cancer Res. 2001; 61 (3): 991-9.

[3] Kemmner W, Wan K, Ruttinger S, Ebert B, Macdonald R, Klamm U, et al. Silencing of human ferrochelatase causes abundant protoporphyrin-IX accumulation in colon cancer. FASEB J. 2008; 22 (2): 500-9.

[4] Wan K, Ebert B, Voigt J, Wang Q, Dai Y, Haag R, et al. In vivo tumor imaging using a novel RNAi-based detection mechanism. Nanomedicine. 2012; 8 (4): 393-8.

[5] Zawacka-Pankau J, Issaeva N, Hossain S, Pramanik A, Selivanova G, Podhajska AJ. Protoporphyrin IX interacts with wild-type p53 protein in vitro and induces cell death of human colon cancer cells in a p53-dependent and -independent manner. J Biol Chem. 2007; 282 (4): 2466-72.

[6] Jiang L, Malik N, Acedo P, Zawacka-Pankau J. Protoporphyrin IX is a dual inhibitor of p53/MDM2 and p53/MDM4 interactions and induces apoptosis in B-cell chronic lymphocytic leukemia cells. Cell Death Discov. 2019; 5: 77.

[7] Zawacka-Pankau J, Kowalska A, Issaeva N, Burcza A, Kwiek P, Bednarz N, et al. Tumor suppressor Fhit protein interacts with protoporphyrin IX in vitro and enhances the response of HeLa cells to photodynamic therapy. J Photochem Photobiol B. 2007; 86 (1): 35-42.

[8] Lee JM, Heo MJ, Lee CG, Yang YM, Kim SG. Increase of miR-199a-5p by protoporphyrin IX, a photocatalyzer, directly inhibits E2F3, sensitizing mesenchymal tumor cells to anti-cancer agents. Oncotarget. 2015; 6 (6): 3918-31.

[9] Carvalho BS, Irizarry RA. A framework for oligonucleotide microarray preprocessing. Bioinformatics. 2010; 26 (19): 2363-7.

[10] Fischer M. Census and evaluation of p53 target genes. Oncogene. 2017; 36 (28): 3943-56.

[11] Matozaki T, Sakamoto C, Suzuki T, Matsuda K, Uchida T, Nakano O, et al. p53 gene mutations in human gastric cancer: wild-type p53 but not mutant p53 suppresses growth of human gastric cancer cells. Cancer Res. 1992; 52 (16): 4335-41.

[12] Dixon SJ, Lemberg KM, Lamprecht MR, Skouta R, Zaitsev EM, Gleason CE, et al. Ferroptosis: an iron-dependent form of nonapoptotic cell death. Cell. 2012; 149 (5): 1060-72.

[13] Rubie C, Kempf K, Hans J, Su T, Tilton B, Georg T, et al. Housekeeping gene variability in normal and cancerous colorectal, pancreatic, esophageal, gastric and hepatic tissues. Molecular and cellular probes. 2005; 19 (2): 101-9.

[14] Livak KJ, Schmittgen TD. Analysis of relative gene expression data using real-time quantitative PCR and the 2 (-Delta Delta C (T)) Method. Methods. 2001; 25 (4): 402-8.

[15] May BK, Dogra SC, Sadlon TJ, Bhasker CR, Cox TC, Bottomley SS. Molecular regulation of heme biosynthesis in higher vertebrates. Prog Nucleic Acid Res Mol Biol. 1995; 51: 1-51.

[16] Elbirt KK, Bonkovsky HL. Heme oxygenase: recent advances in understanding its regulation and role. Proc Assoc Am Physicians. 1999; 111 (5): 438-47.

[17] Shakeri R, Kheirollahi A, Davoodi J. Apaf-1: Regulation and function in cell death. Biochimie. 2017; 135: 111-25.

[18] Leu JI, Dumont P, Hafey M, Murphy ME, George DL. Mitochondrial p53 activates Bak and causes disruption of a Bak-Mcl1 complex. Nat Cell Biol. 2004; 6 (5): 443-50.

[19] Cho H, Chung JY, Song KH, Noh KH, Kim BW, Chung EJ, et al. Apoptosis inhibitor-5 overexpression is associated with tumor progression and poor prognosis in patients with cervical cancer. BMC Cancer. 2014; 14: 545.

[20] Massague J. TGFbeta signalling in context. Nat Rev Mol Cell Biol. 2012; 13 (10): 616-30.

[21] Miyazono K. Transforming growth factor-beta signaling in epithelial-mesenchymal transition and progression of cancer. Proc Jpn Acad Ser B Phys Biol Sci. 2009; 85 (8): 314-23.

[22] Zeng H, Tang L. CRIM1, the antagonist of BMPs, is a potential risk factor of cancer. Curr Cancer Drug Targets. 2014; 14 (7): 652-8.

[23] Yuan CL, Liang R, Liu ZH, Li YQ, Luo XL, Ye JZ, et al. Bone morphogenetic protein and activin membrane-bound inhibitor overexpression inhibits gastric tumor cell invasion via the transforming growth factor-beta/epithelial-mesenchymal transition signaling pathway. Exp Ther Med. 2018; 15 (6): 5422-30.

[24] Briscoe J, Therond PP. The mechanisms of Hedgehog signalling and its roles in development and disease. Nat Rev Mol Cell Biol. 2013; 14 (7): 416-29.

[25] 25. Sun H, Ni SJ, Ye M, Weng W, Zhang Q, Zhang M, et al. Hedgehog Interacting Protein 1 is a Prognostic Marker and Suppresses Cell Metastasis in Gastric Cancer. J Cancer. 2018; 9 (24): 4642-9.

[26] Zhan Y, Zheng N, Teng F, Bao L, Liu F, Zhang M, et al. MiR-199a/b-5p inhibits hepatocellular carcinoma progression by post-transcriptionally suppressing ROCK1. Oncotarget. 2017; 8 (40): 67169-80.

[27] Kim BK, Yoo HI, Kim I, Park J, Kim Yoon S. FZD6 expression is negatively regulated by miR-199a-5p in human colorectal cancer. BMB Rep. 2015; 48 (6): 360-6.

[28] Song H, Hogdall E, Ramus SJ, Dicioccio RA, Hogdall C, Quaye L, et al. Effects of common germ-line genetic variation in cell cycle genes on ovarian cancer survival. Clin Cancer Res. 2008; 14 (4): 1090-5.

[29] Yokota I, Sasaki Y, Kashima L, Idogawa M, Tokino T. Identification and characterization of early growth response 2, a zinc-finger transcription factor, as a p53-regulated proapoptotic gene. Int J Oncol. 2010; 37 (6): 1407-16.